EUROPEAN SPALLATION SOURCE

ESS Instrument Proposal

Project Name	Macromolecular Diffractometer
Date	16/08/2013
Revision	1.3
State	Revised document for SAC review

ESS Instrument Construction Proposal
Macromolecular Diffractometer

	Name	Affiliation
ESS Instrument WP coordinator	Esko Oksanen	ESS
ESS Partners	Esko Oksanen	ESS

The following table is used to track the ESS internal distribution of the submitted proposal.

	Name	Affiliation
Document reviewer	Ken Andersen	ESS
Document approver	Oliver Kirstein	ESS
Distribution (list names)		

European Spallation Source ESS AB
Visiting address: ESS, Tunavägen 24
P.O. Box 176
SE-221 00 Lund
SWEDEN

www.esss.se

OVERVIEW

We propose to build an instrument dedicated to the structure determination of biological macromolecules by crystallography. The scientific driver is to locate the hydrogen atoms relevant for the function of the macromolecule. The proposed instrument is a time-of-flight (TOF) quasi-Laue diffractometer optimised for small samples and large unit cells.
The ESS long pulse source is well suited for a quasi-Laue macromolecular diffractometer that can spread the background in the TOF dimension, while the Bragg peaks are observed at a defined TOF. Therefore a macromolecular diffractometer at the ESS could be used either to study systems with smaller crystals or larger unit cell volumes. Growing well-ordered protein crystals of cubic millimetre volume is extremely difficult, so the instrument is optimised for submillimeter crystal sizes. As the background from incoherent scattering increases dramatically if all ^{1}H cannot be replaced by ^{2}H, the instrument proposed here has a dramatic advantage with systems where perdeuteration cannot be achieved. Many challenging and interesting proteins fall into this category, as they cannot be expressed in prokaryotic systems with high enough yield.
One of the limiting factors with current instruments is that the fixed detector geometry only allows a maximal unit cell edge of ~150 Å to be resolved without a compromise in the diffraction resolution (d_{min}). The instrument proposed here allows larger unit cells to be resolved by increasing the crystal-to-detector distance, albeit which incurs an increase in the data collection time, but reflections to the same d_{min} can still be observed by swinging the detector in 2θ angle. Many of the scientifically most interesting systems, such as proton pumping membrane proteins, crystallise in large unit cells, so simply being able to resolve a large unit cell edge is a unique advantage. The combination of a neutron flux comparable to leading high flux reactor instruments, such as LADI-III, together with time-of-flight expansion, the ability to resolve large unit cells and the ability to separate signal from background leads to world-leading performance particularly with the experimentally most challenging systems. This would transform NMX into a technique that could answer a significantly larger number of hydrogen related questions in biomolecular science than before.
The proposed instrument can also be used to study materials science by single crystal diffraction – particularly in the field of magnetism – even before dedicated instruments are available at the ESS for all scientific communities.

TABLE OF CONTENTS

1. INSTRUMENT PROPOSAL

1.1 Scientific Impact

The proposed instrument is a single crystal diffractometer specially optimised for structural studies of biological macromolecules. In addition to this main scientific driver in structural biology, the instrument can be used for studies in other fields of science such as materials research.

1.1.1 Structural Biology

The main scientific drivers for neutron macromolecular crystallography (NMX) involve the determination of hydrogen atom positions, for example to elucidate enzyme mechanisms, understand protein-ligand interactions in detail or to visualize proton transport across biological membranes. Hydrogen atoms play a key role in many fundamental chemical processes of living cells, but the standard structure determination methods such as X-ray crystallography cannot consistently determine their locations. NMX is therefore of wide scientific interest for structural biology and biochemistry.

Enzymes are biological catalysts that are essential for all the processes of living cells, but they are also increasingly used for industrial processes. Most enzymatic reactions involve transfers of hydrogens, but our understanding of enzymatic catalysis is limited by the lack of information about the hydrogen positions in various stages of the reaction cycle. NMX would yield a deeper understanding of enzyme action and help in engineering better industrial enzymes.

Most proteins that catalyse or regulate biologically important redox reactions use metal cofactors. An important advantage of NMX compared to X-ray crystallography is the absence of photoreduction, allowing the metalloproteins to be studied in the truly oxidised state.

The detailed molecular interactions between proteins and small molecule ligands are crucial in structure-based drug discovery and the positions of the hydrogen atoms are an important

input particularly for computational studies of pharmaceutical binding. This could lead to significant advances in the development of new pharmaceuticals.

Energy transduction in biological system is based on proton gradients across biological membranes, and the membrane proteins that generate and use these gradients are indispensable for all life. Membrane protein crystallography is experimentally very challenging and neutron studies of membrane proteins have so far not been reported, but such studies would have a very high scientific impact.

While NMX is conceptually very similar to X-ray crystallography that has become a standard method in biochemistry, it remains experimentally so challenging that the number of systems studied so far is very limited. The limiting factors are beamtime availability on one hand and the need for relatively large and preferably perdeuterated crystals on the other hand. Because of the intrinsically high background from the crystal and the surrounding mother liquor, macromolecular crystallography is limited by the signal-to-noise ratio. The ESS long pulse source is well suited for a quasi-Laue macromolecular diffractometer that can spread the background in the time-of-flight (TOF) dimension, while the Bragg peaks are observed at a defined TOF (see below). This makes the most of the source spectrum while essentially retaining the advantage of monochromatising the beam. Therefore a macromolecular diffractometer at the ESS could be used either to study systems with smaller crystals or larger unit cell volumes. As the background from incoherent scattering increases dramatically if all ^{1}H cannot be replaced by ^{2}H, the instrument proposed here has dramatic advantage with systems where perdeuteration cannot be achieved. Many challenging and interesting proteins fall in this category, as they cannot be expressed in prokaryotic systems with high enough yield.

One of the limiting factors with current instruments is that the fixed detector geometry only allows a maximal unit cell edge of ~150 Å to be resolved without a compromise in the diffraction resolution (d_{min}). The instrument proposed here allows larger unit cells to be resolved by increasing the crystal-to-detector distance, which incurs an increase in the data collection time, but reflections to the same d_{min} can still be observed by swinging the detector about the 2θ angle. Many of the scientifically most interesting systems, such as proton pumping membrane proteins, crystallise in large unit cells, so simply being able to resolve a large unit cell edge is a unique advantage. The combination of flux comparable to leading reactor instruments such as LADI-III, the ability to resolve large unit cells and the ability to separate signal from background leads to world-leading performance particularly with the experimentally most challenging systems. This would transform NMX to a technique that could answer a much larger number of hydrogen related questions in biomolecular science than before.

1.1.2 Materials Research

The proposed instrument can be used to study any single crystal material with a large periodicity. The periodicity does not need to be the nuclear unit cell, but may arise from *e.g.* superlattices or incommensurate modulation. While inorganic materials with large unit cells, such as metal-organic frameworks, are of wide interest, single crystals of the size and quality required for neutron studies are rarely available. A very promising use of the proposed instrument, on the other hand, is in the study of magnetic materials.

Many magnetic materials exhibit long-range features in length scales much larger than the structural unit cell. Examples include Dirac strings separating magnetic monopoles in spin ices, changes in magnetic structure upon charge ordering in ferroelectrics and magnetic

vortices and skyrmion lattices. Such phenomena typically manifest themselves in the diffraction pattern as either closely separated satellite peaks or weak features over a large background – situations not dissimilar to macromolecular diffraction. The magnetic form factors fall off rapidly with the momentum transfer **q**, so the wavelength range available from a cold moderator is well suited for studies of magnetism. Polarised neutron beams can be used for magnetic diffraction experiments to observe weak features obscured by *e.g.* nuclear Bragg reflections. The high spatial resolution and flexibility of the detector geometry will allow weak magnetic scattering signals to be extracted especially if the nuclear scattering can be modelled reliably.

Macromolecular crystallography is most often limited by the sample volume that can be obtained. This situation is very similar for studies of materials at extreme environments, particularly high pressure. The volumes achievable in a diamond anvil cell are very similar to the samples the proposed instrument is optimised for. The instrument could therefore be used for single crystal and even powder diffraction studies under high pressures, before a dedicated instrument is available for this purpose.

1.2 User Base and Demand

Macromolecular X-ray crystallography is a key technique in biochemistry and most bioscience institutes include research groups using crystallography. This in Europe alone means several hundreds of groups, who constitute a major user group of synchrotron sources. For example 15% of the scheduled beamtime at the European Synchrotron Radiation Facility (ESRF) was for macromolecular crystallography. Macromolecular neutron crystallography is conceptually very similar to X-ray crystallography and crystallographers are already used to travel to large-scale facilities, so the potential user base includes thousands of researchers. The limited availability of instruments combined with long measurement times and the requirement for large crystals with small unit cells has limited the number of X-ray crystallographers using neutron diffraction. A large number of proteins where neutron crystallography could offer important insights crystallise with unit cells that are prohibitively large for current instruments to resolve. While many of the recent NMX structures have been published in PNAS or similar journals, almost every issue of Nature and Science contains a paper using X-ray macromolecular crystallography and in the last ten years four Nobel prizes have been awarded to macromolecular crystallographers (MacKinnon 2003, Kornberg 2006, Ramakrishnan, Steitz & Yonath 2009 and Lefkowitz & Kobilka 2012). Enlarging the scope of NMX to larger systems and particularly membrane proteins could lead to very high impact publications. The systematic use of NMX to study protein-ligand interactions is of significant interest to the pharmaceutical industry. Industry involvement can be envisaged through both proprietary research beamtime and industrial-academic partnerships.

The requirement for perdeuterated protein and large crystals is an obstacle for many potential users, which accentuates the need for appropriate supporting facilities for perdeuteration and large crystal growth. All of the potential users are not experts in protein production and the specific techniques of perdeuteration, so an ESS bio-deuteration facility is necessary for the success of an NMX instrument. The small beams and rapid data collection in X-ray crystallography have led to a situation where the crystallization methods are optimized for crystals of ~50-200 μm size, even though larger crystals can be grown in slightly different setups. The data collection time is also proportional to crystal volume, and any improvement in crystal volume and quality directly impacts the required measurement time. Therefore a crystallisation facility that helps users to grow the largest possible crystals using the best technology available is a crucial complement to this instrument.

If NMX does become a widely used technique among macromolecular crystallographers, one instrument at the ESS might become heavily oversubscribed. As only a small part of the moderator phase space can actually be used by one instrument, the design will allow more than one small cross section, low divergence beam to be extracted from the same beamport. This leaves open a range of upgrade possibilities, including the construction of additional NMX instruments without requiring a new beamport.

The concept presented here is optimised for systems that currently cannot be feasibly studied by NMX either due to a large unit cell or small crystals available, particularly in cases where perdeuteration of the protein cannot be achieved. The gain in instrument performance from the intense ESS pulse and background reduction is therefore used to expand the scope of science accessible compared to existing instruments elsewhere.

The instrument will serve the needs of the chemical crystallography community for large unit cells as well as the magnetic single crystal diffraction community. Such experiments can produce high scientific impact already in the early years of ESS before dedicated instruments are available. In the longer term the instrument will be complementary to the rest of the ESS diffraction instrument suite for specific experiments that benefit from the flexible detector geometry and high spatial resolution.

1.3 Description of Instrument Concept and Performance

In the Laue method large number of reflections are simultaneously excited, thus allowing much more rapid data collection than with the monochromatic oscillation method commonly used in macromolecular X-ray crystallography. This, however, results a high density of spots that are experimentally challenging to resolve. In addition a fraction (up to 12.5 % (Cruickshank, Helliwell & Moffat (1987) *Acta Cryst.* A**43**, 656-674)) of the Laue spots contain more than one reflection, known as harmonic overlap. This limits the achievable completeness of a data set.

Another aspect of the Laue method is that the signal is only recorded at a narrow wavelength range for any one reflection, while the background is to a first approximation uniformly distributed over the entire wavelength range. Using the TOF information available at a pulsed source instrument all of these problems can be significantly mitigated.

Choice of moderator

The instrument proposed here is a single crystal quasi-Laue TOF diffractometer optimised for submillimeter crystals with large unit cells. The main scientific driver is to determine the positions of hydrogen atoms in biological macromolecules, which requires $d_{min} \lesssim 2.5$ Å and the diffraction limit of protein crystals used in NMX is typically 1.5-2.5 Å. Choosing the wavelength range is therefore a compromise between an acceptable d_{min} and higher signal available with colder neutrons. While longer wavelength neutrons are scattered more efficiently by the crystal, they scatter at a higher angle for a given d-spacing. This is advantageous for separating the diffraction spots in large unit cells, but it also means that a larger solid angle coverage is necessary to cover reciprocal space to the diffraction limit of the crystal. Another consideration is the available neutron flux at different wavelengths, which has to be weighted by the wavelength dependence of detector efficiency.

The wavelength range proposed for this instrument is centered at 2.65 Å and as a result of the chosen instrument length (as discussed below) ranges from 1.8 Å to 3.55 Å. This matches well with the spectrum of the cold moderator at the ESS, although the spectrum is not symmetric around the maximum at ~2.6 Å, and higher brightness at shorter wavelengths where detector efficiency is expected to be lower would be preferable. It is possible that there are regions of the moderator that have an optimal spectrum, but at this time there is limited information available. All the ESS beamports can view both the cold and thermal moderators without a significant change in the in-monolith optics, so the instrument will view the part of the moderator providing the highest intensity for the chosen wavelength range. It is also worth noting that the chopper system proposed (see below) allows the wavelength range to be tuned or even narrowed down by simply rephasing the choppers, which in turn allows tailoring the wavelength band in each experiment.

Instrument length and layout

The instrument concept proposed here uses the full time width of the ESS source pulse, but only a limited wavelength band. The moderator-to-sample distance that defines the available wavelength band is 156 m. This allows a wavelength band of 1.74 Å and a nominal wavelength resolution ranging from 4.0% at 1.8 Å to 2.0% at 3.55 Å using the full 2.86 ms source pulse. While limiting the wavelength band does reduce the available neutron flux ~35% compared to *e.g.* a 3.6 Å bandwidth for a 75 m instrument, it is also the approach

used at continuous source instruments such as LADI-III to avoid reflection overlap. With the 1.74 Å bandwidth 94.6 % of the spots are expected to contain just one reflection, whereas with a 3.6 Å bandwidth only 88.4 % of the spots are expected to be singles (Cruickshank, Helliwell & Moffat (1987) *Acta Cryst.* A**43**, 656-674, Table 4.)

As shown below, the wavelength information from the neutron TOF allows both spatial and harmonic overlaps to be resolved. Making the instrument longer both reduces the number of harmonic overlaps (as the bandwidth get narrower) and improves the ability to resolve them (as the wavelength resolution improves). The instrument length is therefore a compromise between available flux and the achievable completeness of a data set for a given unit cell size.

The main advantage, however, of the TOF separation in quasi-Laue crystallography is spreading the background in multiple time bins compared to the continuous quasi-Laue method.

The wavelength resolution could be improved by using a pulse shaping chopper that reduces the effective pulse time-width, but also the available flux. A practical limitation for pulse-shaping choppers is that they have to be placed outside the target monolith at 6 m from the moderator, where the time width of the pulse is already broader. This means that a pulse shaping chopper with an opening >120 μs inevitably functions as a bandwidth chopper as well, leading to further intensity losses in useful wavelengths. In order to make full use of the intense long pulse, no pulse shaping chopper is used, limiting the achievable wavelength resolution, but reducing the cost and complexity of the instrument.

The geometry proposed here allows diffraction spots to be separated spatially as much is necessary for reliable integration by changing the detector distance. A precondition is that the angular width of the reflection that is determined by the crystal mosaicity and beam divergence does not exceed the angular separation between reflections. This underlines the requirement for well-ordered crystals for large unit cell systems. This is also why the beam divergence needs to be matched to the crystal mosaicity when it exceeds ~0.1°. Otherwise the beam divergence can be adjusted to allow a sufficient angular separation along the largest unit cell dimension.

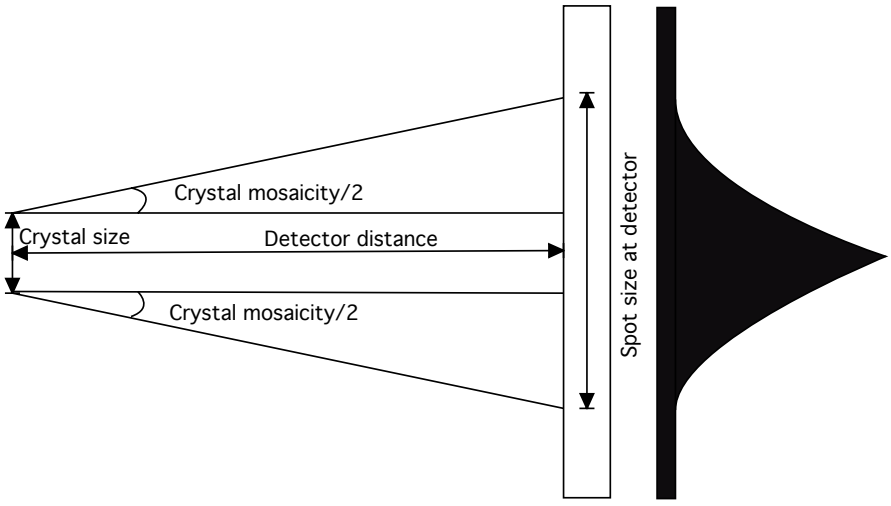

Figure 1 Determination of the spot size at the detector. The reflection is assumed to be perpendicular to the detector plane.

Another precondition is that the size of the diffraction spot on the detector, defined by the size of the crystal, the size of the neutron beam and the angular width of the reflection (which we assume to be determined by the crystal mosaicity) is smaller than the separation of the reflection centroids. This requires a sufficient spatial resolution as discussed below. It is also helpful that the angular separation between adjacent reflections increases with the wavelength (and hence scattering angle for a given Miller index), with the consequence that reflections that are overlapped at smaller scattering angles and shorter wavelengths can still be resolved at higher scattering angle and longer wavelength. The limitation then becomes the accessible scattering angle and the time required to collect a complete data set. The flexible detector geometry allows many different strategies to be used, which calls for efficient and easy-to-use software for optimising the data collection strategy.

Besides being resolved in the two spatial dimensions on the detector, the diffraction spots can be resolved also by the time-of-flight. As discussed below the ~4 ms effective time width of the reflections is significantly smaller than the time separation between the reflections in a given detector pixel, provided that the pixels are sufficiently small. The time width of a reflection is also still only a small fraction of the total 71.4 ms time frame, whereas the background in each pixel is spread over the entire frame. It is also worth noting that the time separation between adjacent reflections increases with the d-spacing, so the lower order reflections that are more difficult to separate in the spatial dimension are in many cases separable by TOF.

Beam delivery system

The beam characteristics will be tailored to the crystal properties, namely matching the beam size with crystal size and beam divergence with crystal mosaicity. As well-ordered protein crystals typically have low mosaicities, the maximum divergence that could be used is ~±0.2°. The beam extraction and delivery system is adapted to these requirements. A 3 cm wide neutron guide of square cross-section will begin 2 m from the moderator surface. The guide will be continuously curved with a radius of 26.84 km to be out of direct line-of-sight of the moderator at 80 m distance. The small beam size required at the sample and the modest divergence that can be accepted without impairing the ability to separate reflections in scattering angle mean that a simple nickel coating (m-value 1) is sufficient on three faces of the guide. On the vertical face on the outward side of the curvature slightly higher reflection angles are needed and a supermirror coating with an m-value of 1.8 will be used. The use of low m-value coating not only reduces the cost, but also provides efficient beam transport due to the high reflectivity below the critical angle. The guide will end at 148.5 m from the moderator and is followed by an adjustable slit collimation system that allows the beam size and divergence to be chosen at will. The last slit that defines the beam size will be placed immediately next to the sample. The collimating optics can be interchanged with a focussing nose that allows a higher flux to be delivered at the crystal at the expense of increased divergence. This option will be useful for crystals with small unit cell dimensions where a larger divergence can be accepted while still separating the reflections. A polarising supermirror can easily be installed at a sufficient distance from the sample for polarisation of the incoming beam.

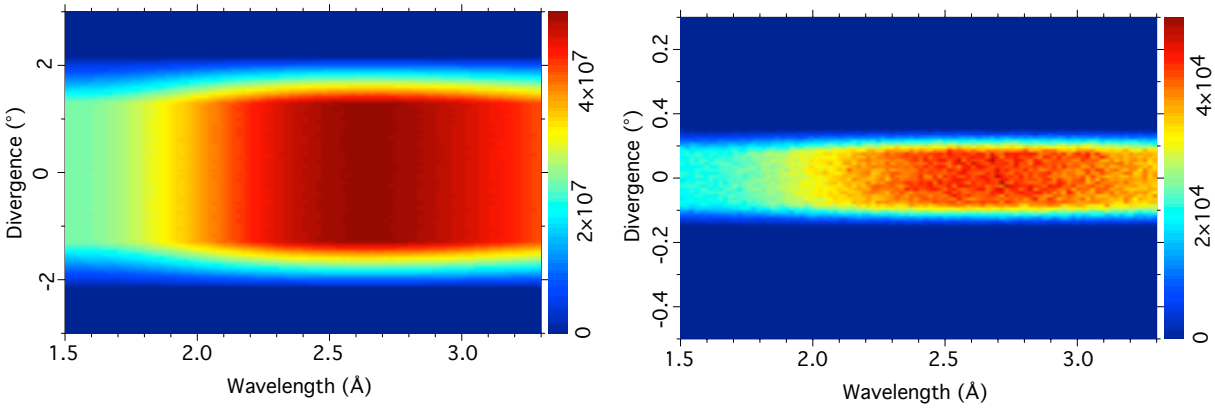

Figure 2 Simulated beam divergence as function of wavelength at A) the start of the guide B) at the sample position.

For a typical beam divergence of ±0.1°, the time-averaged flux at the sample is expected to be ~3x10^8 neutrons/s/cm^2 for the cold source, assuming >90% brilliance transfer. As the latest moderator spectral brilliance curves have not yet been implemented in the McStas package, a direct comparison with Monte Carlo simulations could not be performed, but the simulation results agree within the uncertainty in the moderator brilliance. This flux is significantly higher than the measured flux of 9.7x10^6 neutrons/s/cm^2 at the PCS[1] (Langan, P. *et al.* (2004) *J. Appl. Cryst.* **37**, 24-31) and somewhat higher than the measured flux of 5x10^7 neutrons/s/cm^2 at LADI-III at its new H143 position for a 3-4 Å wavelength range (Blakeley, M. *personal communication*).

While there is no pulse shaping chopper, the bandwidth selection and frame overlap rejection will nonetheless be achieved by a chopper system consisting of two double disc choppers rotating at the 14 Hz source frequency and located at 20 m and 50 m from the moderator. The double disc setup allows the chopper opening time to be changed by rephasing the two discs, which allows the tailoring of the wavelength band to match the unit cell size and diffraction limit of each crystal. The chopper system is optimised to give the highest possible transmission of the useful wavelength range, even at the expense of wavelength contaminations. These can be tolerated as the reflections are spatially separated on the detector and the contaminations can be taken into account in predicting reflection positions for integration. The frame overlap that results from long wavelength neutrons from a previous pulse to be accepted by the bandwidth choppers is not a serious problem for macromolecular crystallography, as relatively few reflections will be observed with λ>15 Å. The proposed chopper system will, however, suppress frame overlap up to 29 Å.

Sample position

The goniostat system has to position the crystal in the beam and change its orientation with a mechanical precision in the micrometer range. One of the practical problems in neutron data collection using longer wavelengths than typically for X-rays is that the Ewald sphere is small and hence the 'blind zone' is relatively large particularly at long d-spacings. In order to obtain good completeness especially at low resolution, several different orientations of the crystal are often needed. Using an industrial six-axis robotic arm as the goniostat allows

[1] It should be noted that up to 20% of the useful neutrons lie outside the 1-5Å wavelength range used for the measurement.

defining the crystal orientation and together with an efficient data collection strategy program it allows the strategy to be optimally implemented. The robot can also be used as a sample changer, increasing the throughput of the instrument. It would also allow X-ray data to be collected by an X-ray generator at the instrument at exactly the same crystal orientation(s). Room temperature X-ray data collection from the same crystal is crucial for the joint crystallographic refinement, so an X-ray diffractometer has to be available either directly at the instrument or in a laboratory within the controlled zone.

The sample area will be designed to accommodate appropriate ESS sample environment equipment – such as cryostats or pressure cells – for material science experiments. The flexible detector geometry also allows compact electromagnets or shielded cryomagnets to be used.

Detector system

The detector system consists of three 60 x 60 cm detector units that can be translated along the sample-detector axis. That axis can then be rotated about the 2θ angle, such that the detectors cover a continuous range in solid angle in the normal situation. In some cases the detector distances could be changed individually for example to collect low-resolution data at low scattering angle.

In order to reliably integrate reflection intensities by profile fitting, the diffraction spots have to be observed in multiple detector pixels. With crystal sizes ~0.3 mm, the spot sizes (Figure 1) are still <1 mm, which calls for a ~0.2 mm spatial resolution to spread the spots over several pixels. This value is consistent with the 0.25 mm readout pixel size typically used at *e.g.* LADI-III. The active detector area of 1.08 m^2 with 0.2 mm pixel size gives rise to a total of 27 million pixels. The flexibility in detector geometry allows a solid angle coverage comparable to LADI-III at a short detector distance (Figure 3, left) and the possibility to resolve very large unit cells by increasing the detector distance (Figure 3, right). The time resolution required from the detector units is only in the order of 1 ms, which is not a limiting factor for the technologies proposed (see below).

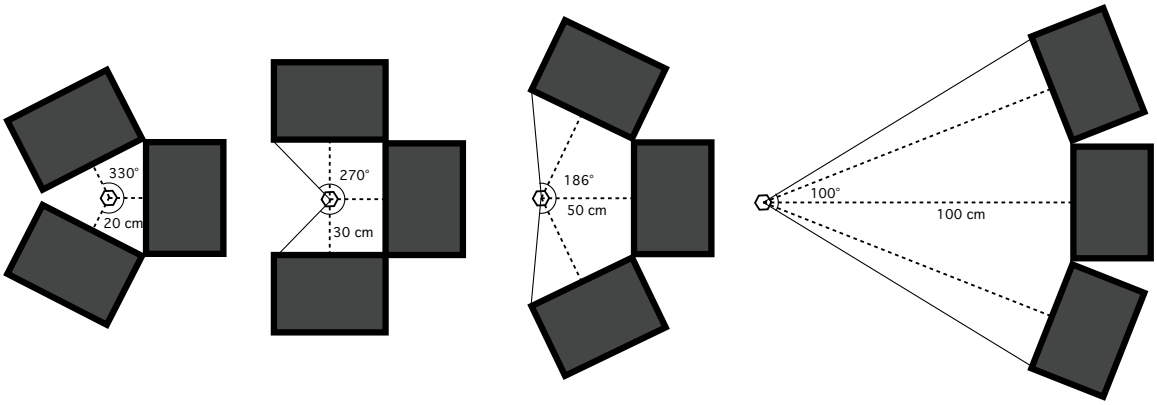

Figure 3 The detector geometry illustrated as a function of crystal-detector distance and the total scattering angle covered in the horizontal plane.

Instrument simulations

Simulating complete diffraction patterns from larger unit cells with the McStas Monte Carlo package has proven challenging and hence a hybrid approach was adopted. Using simulated Laue patterns of the potassium channel NaK (space group I_4, a=b=67.95 Å, c=89.64 Å) from

the program Lauegen (**Figure 4**), small areas of reciprocal space containing both harmonically and spatially overlapped reflections were identified and the 52 reflections in that region were simulated with arbitrary intensities. These simulations are consistent with the ~4 ms time width of the reflections (Figure 5) that was expected.

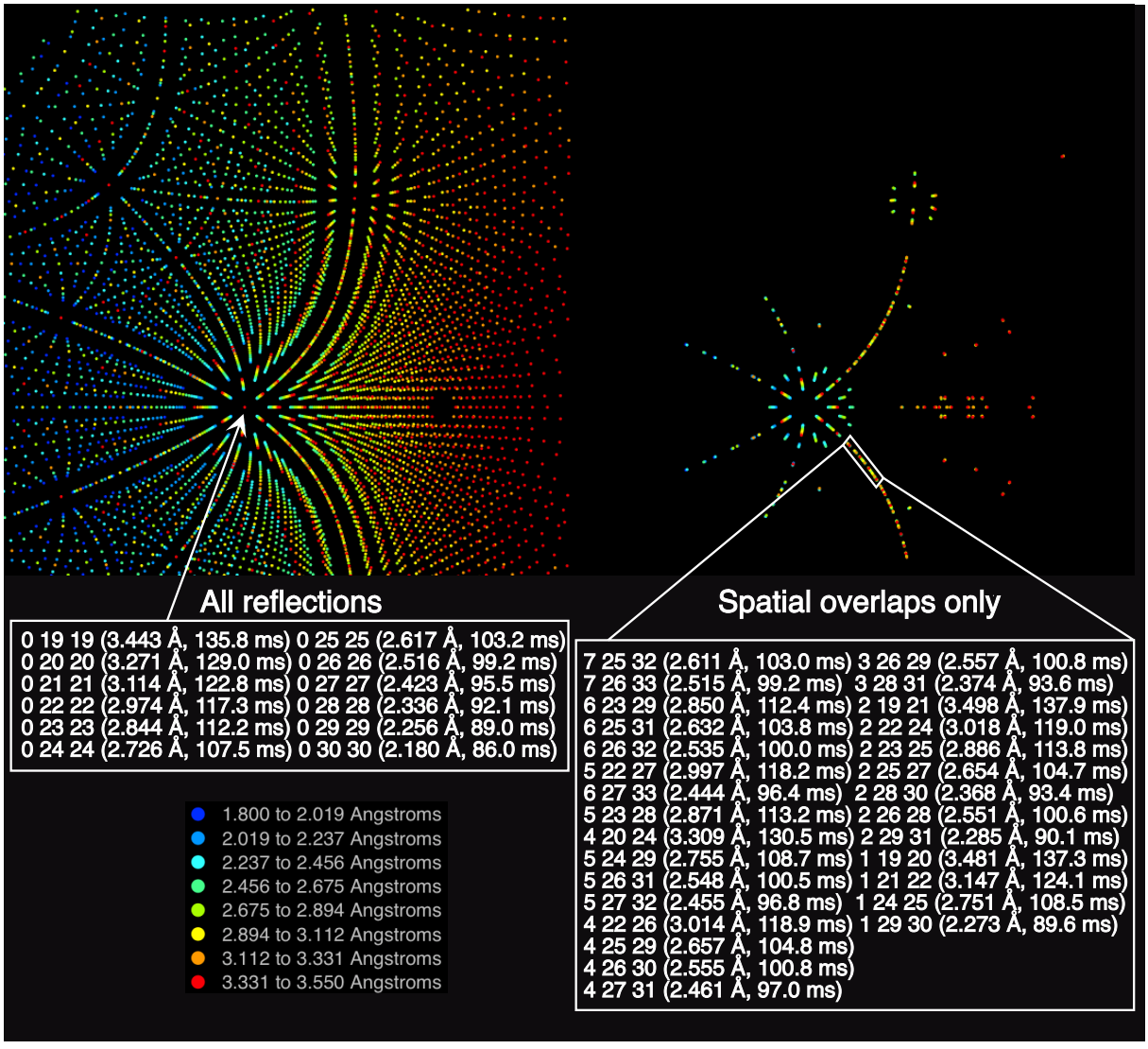

Figure 4 Simulated Laue pattern (2θ = 120°, detector distance 200 mm) from the potassium channel NaK (a=b=67.95 Å, c=89.64 Å) with example harmonic (left) and spatial (right) reflections highlighted.

The effect of the detector point spread function was investigated by convoluting the simulated reflections from a 0.5 x 0.5 mm crystal with 0.1° mosaicity of the potassium channel NaK with various point spread functions (Figure 6). The functions used were two-dimensional Gaussians with a standard deviation of 0.2, 0.5 and 1.0 mm respectively. As might be expected a point spread function with a standard deviation smaller (0.2 mm) or comparable (0.5 mm) to the crystal size have little effect on the observed spot size (Figure 6, 3 first panels). A larger (1.0 mm) spread has a much more noticeable effect (Figure 6, right panel), even though it doesn't yet preclude separating the spots using the TOF

information in this example (Figure 6, bottom). For smaller crystals and more closely spaced reflections the effect will be more pronounced.

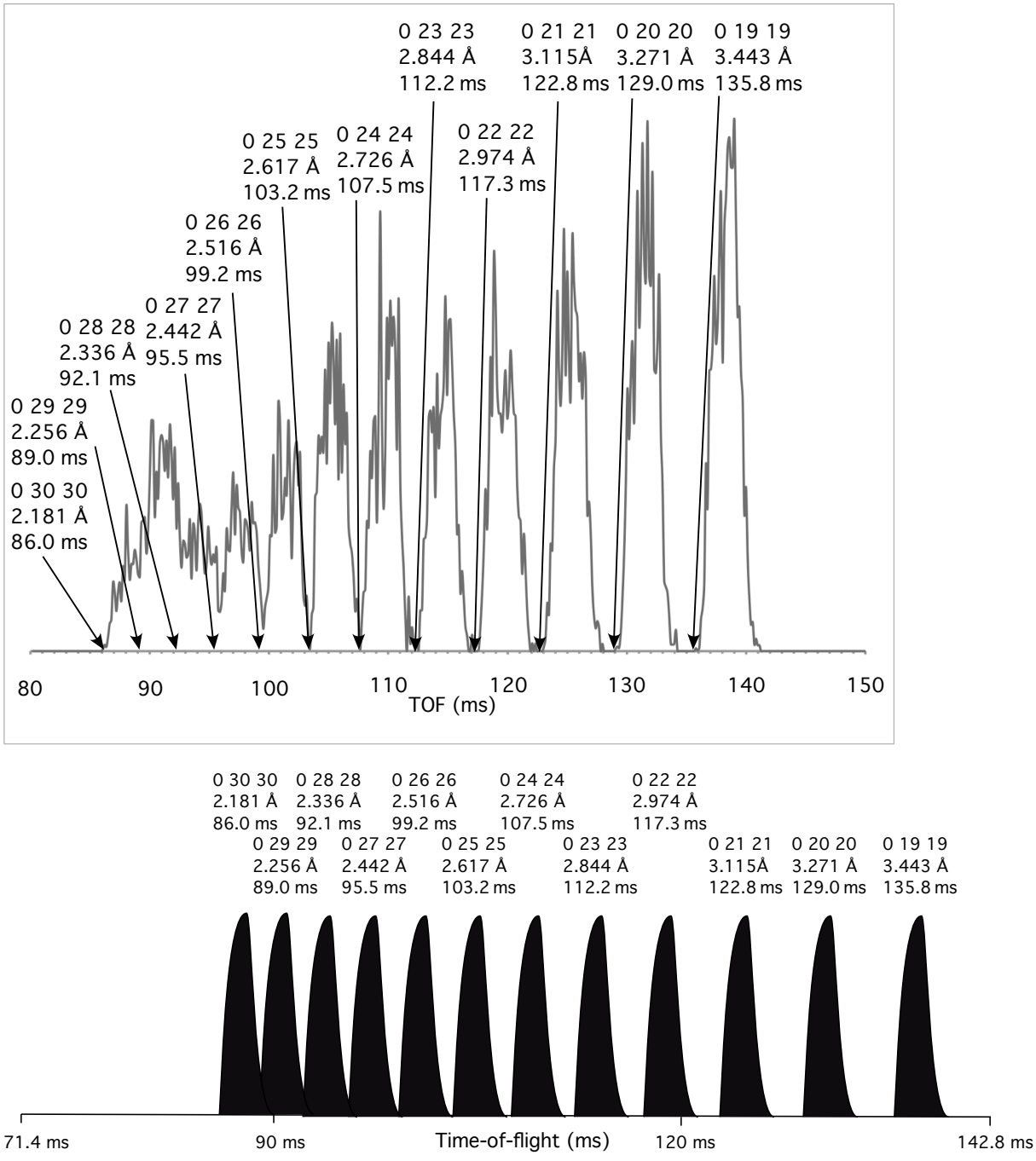

Figure 5 The simulated (top) and scale drawing (bottom) representing TOF separation of the harmonically overlapped reflections 0 19-30 19-30 using arbitrary reflection intensities. The time width in the scale drawing is 4 ms.

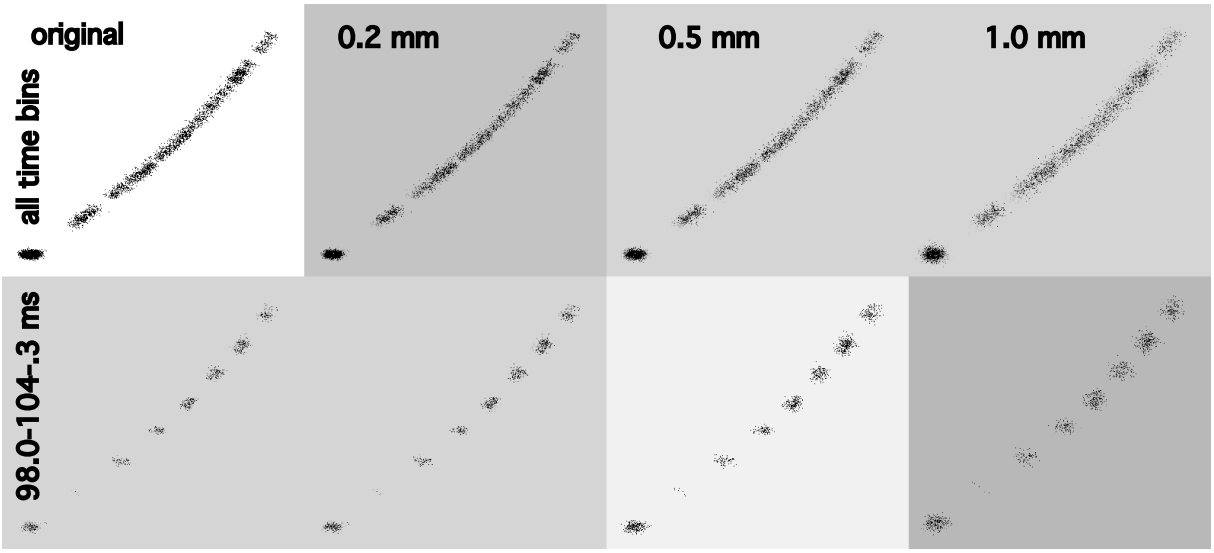

Figure 6 Simulated diffraction patterns from example reflections above convoluted with Gaussian point spread functions of 0.2, 0.5 and 1.0 mm standard deviation. The top panel shows all time bins and the bottom panel a ~6 ms time window.

Instrument performance

The performance gain over existing instruments depends very heavily on the individual crystal and is therefore difficult to quantify exactly. The quasi-Laue time-of-flight method combines the advantage of the Laue method for making efficient use of the neutron flux over a reasonably wide spectrum and the advantage in signal-to-noise of the monochromatic method. This makes the concept inherently well suited to a long-pulse source such as the ESS.

Let us consider a crystal of a given diffracting power in a polychromatic neutron beam of a given flux in the absence of any background from the crystal or its surrounding mother liquor. For a single Laue spot the counting time required to reach a given signal-to-noise ratio is essentially defined by the spectral flux at the wavelength where the reflection is excited and the detector noise. Then the time required to reach acceptable counting statistics would be the same regardless of whether any wavelength resolution (TOF) is used. If, however, we take into account the background, the counting time needed for a given signal-to-noise ratio in the absence of wavelength resolution (conventional Laue) becomes a function of the spectral flux (and detector efficiency) at all the wavelengths within the wavelength range where background is generated and the integral of that background across the wavelength range used. In the case of using the TOF information as well, the counting time is defined by the background *only* at the wavelength where the reflection is excited. If we assume the background to be fairly uniform across the wavelength range, the gain factor over a continuous source Laue instrument of similar time averaged flux (such as LADI-III) depends very strongly on the level background from the sample. With the concept proposed here the time width of a reflection is ~4 ms, which is 6 % of the 71.4 ms timeframe. This means that the effective background is lowered by a factor of ~20 by using the TOF method. In macromolecular crystallography the background from the crystal and its surroundings is typically very much larger than the actual Bragg peak heights, especially for the weakest reflections that define the required counting time. Therefore the impact of lowering the effective background is most pronounced for large unit cells where the average

intensity of reflections falls rapidly with resolution. The implication is that a counting time required for the same crystal can be reduced by a factor of ~20 or – more importantly – a crystal 20 times smaller can be used. This represents a conservative estimate of the performance gain, as *e.g.* no improvements in detector efficiency or reductions in γ-background have been considered.

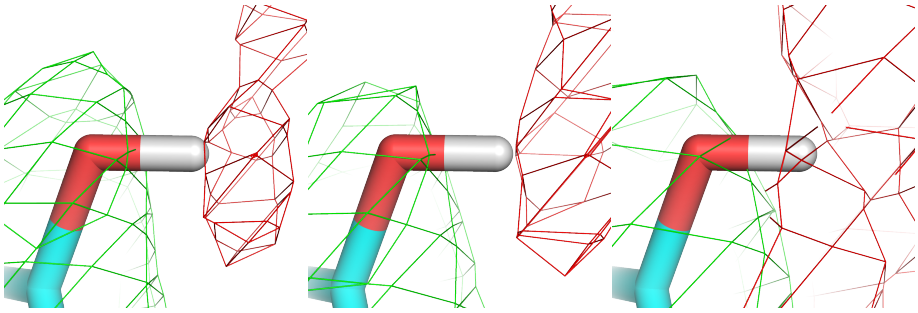

Figure 7 Calculated nuclear scattering length density maps contoured at 1σ (positive green ,negative red) of the phenol group of Tyr244 of Thermus thermophiles cytochrome c oxidase calculated at A) 1.5 Å B) 1.8 Å and C) 2.3 Å resolution.

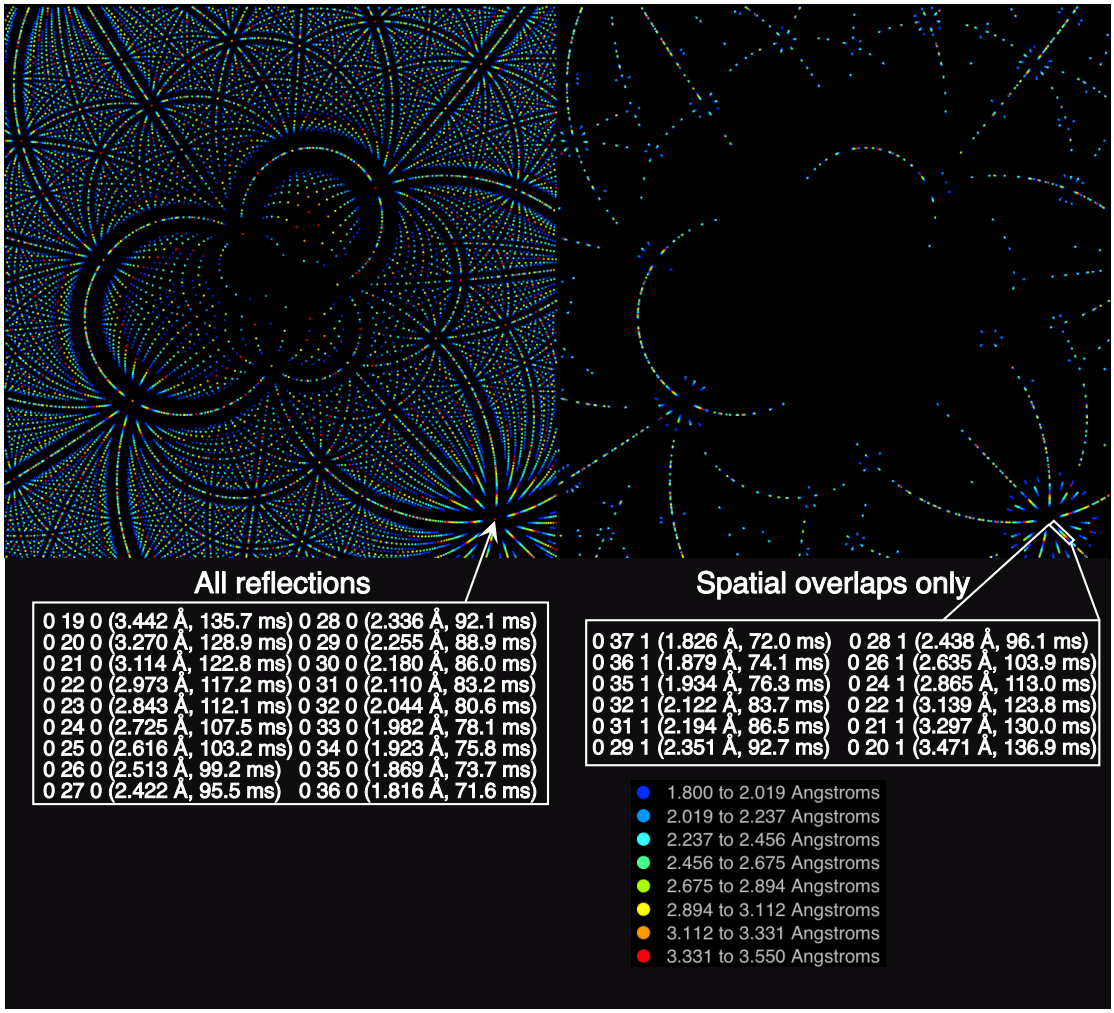

Figure 8 Simulated Laue pattern from the sarcoplasmic reticulum calcium ATPase with example harmonic (left) and spatial (right) reflections highlighted.

The lowering of the effective background is especially important if full deuteration of the sample cannot be achieved and it may even be feasible to study fully hydrogenated samples, even though that requires not only longer counting times, but also sufficient diffraction resolution (Figure 7) to avoid cancellation of the negative and positive peaks from ^{1}H and heavier elements respectively.

A simulated Laue pattern by the program Lauegen from the membrane protein sarcoplasmic reticulum calcium ATPase (**Figure 8**), with the unit cell dimensions a = 101.93 Å b = 109.42 Å c = 276.09 Å illustrates how the instrument concept would perform with a reasonably large unit cell. The criterion for spot overlap of 1.5 mm (spot_delta in Lauegen) is chosen by the calculated spot size of 1.4 mm assuming a crystal size (and hence beam size) of 0.5 mm, angular width of ±0.1° and detector distance of 500 mm at $2\theta = 0°$. In this arbitratry crystal orientation 1518 out of 13616 total spots are considered overlapped by this criterion. Therefore ~90% of the reflections can be separated in the spatial dimension alone, excluding also the possibility of spatial overlap deconvolution, which would further reduce the number of reflections that cannot be integrated without using the TOF information.

Example reflections of harmonic overlaps (left) and spatial overlaps (right) are shown with the wavelengths at which the reflection is observed and the time-of-flight. The 2.86 ms source pulse imposes a ~4 ms full width in TOF for any given wavelength, but it should be noted that even when the difference in TOF between adjacent reflections is < 4 ms (such as 0 35 0 and 0 36 0), deconvolution could still be feasible as the pulse shape is known. This is illustrated by a scale drawing (Figure 2) of the 71.4 ms timeframe with the harmonically (top) and spatially (bottom) overlapped example reflections shown in Figure 1. Each reflection is represented by a peak (qualitatively resembling the shape of the ESS pulse) with a full width of 4 ms.

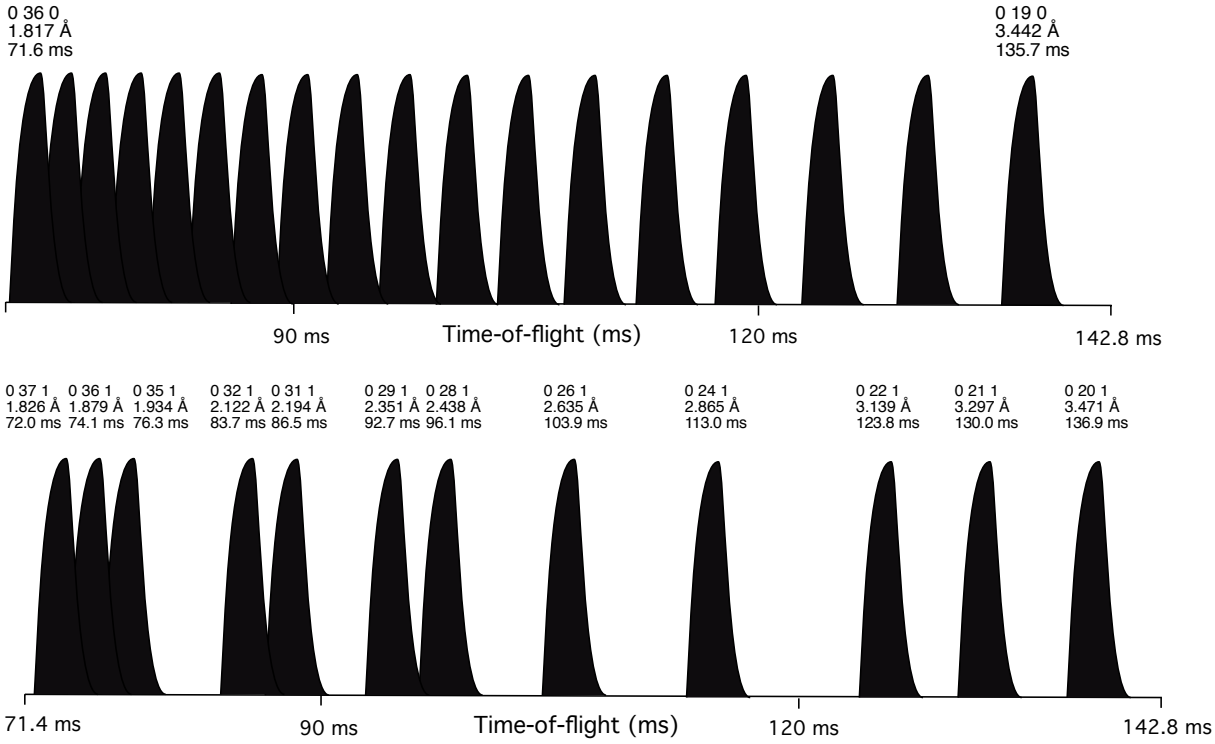

Figure 9 Scale drawing representing the time-of-flight separation of the harmonically (top) and spatially (bottom) overlapped example reflections in SERCA.

When the unit cell is sufficiently large, such as bovine heart cytochrome c oxidase (Figure 10) with unit cell dimensions a = 182.59 Å b = 205.40 Å c = 178.25 Å (in space group $P2_12_12_1$), a large fraction of the reflections become spatially overlapped even at the maximal detector distance of 1000 mm. With a crystal size (and hence beam size) of 0.5 mm and an angular width of ±0.1°, the spot size on the detector is calculated to be 2.3 mm. At 2θ = 45° and a spot overlap criterion of 2.4 mm, 19224 of 32550 reflections are considered spatially overlapped. While resolving the harmonically overlapped reflections (

Figure 11) in such unit cells would require some deconvolution method, the spatially overlapped reflections can often still be resolved in the spatial dimension. For example all the reflections that overlap in the TOF dimension in lower panel of Figure 11 such as (27 52 79), (28 53 78) and (27 52 77) are in fact spatially well separated (Figure 12). This illustrates the capability of the proposed instrument to resolve fairly large unit cells using the full pulse width.

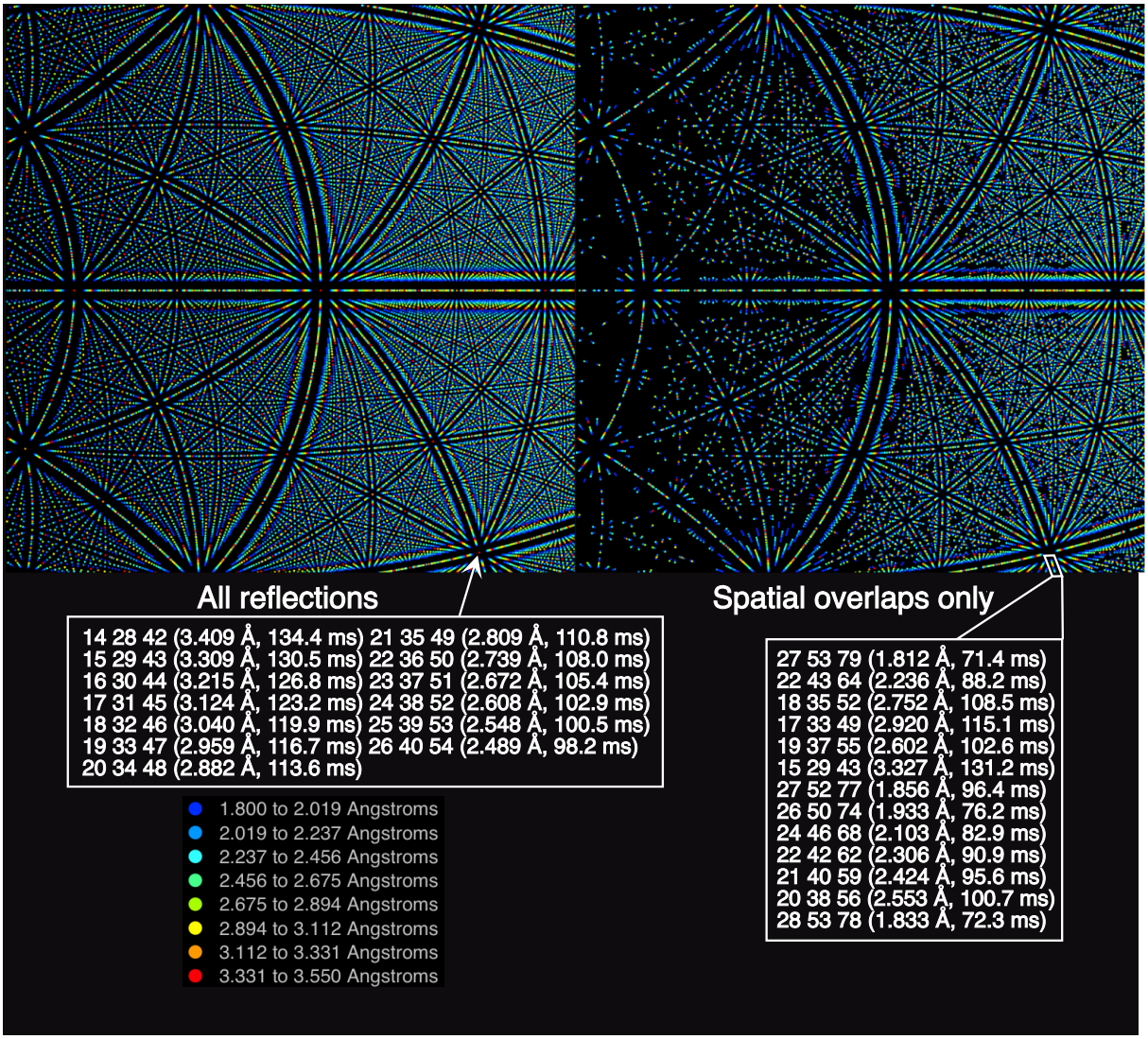

Figure 10 Simulated Laue pattern from bovine heart cytochrome c oxidase with example harmonic (left) and spatial (right) reflections highlighted.

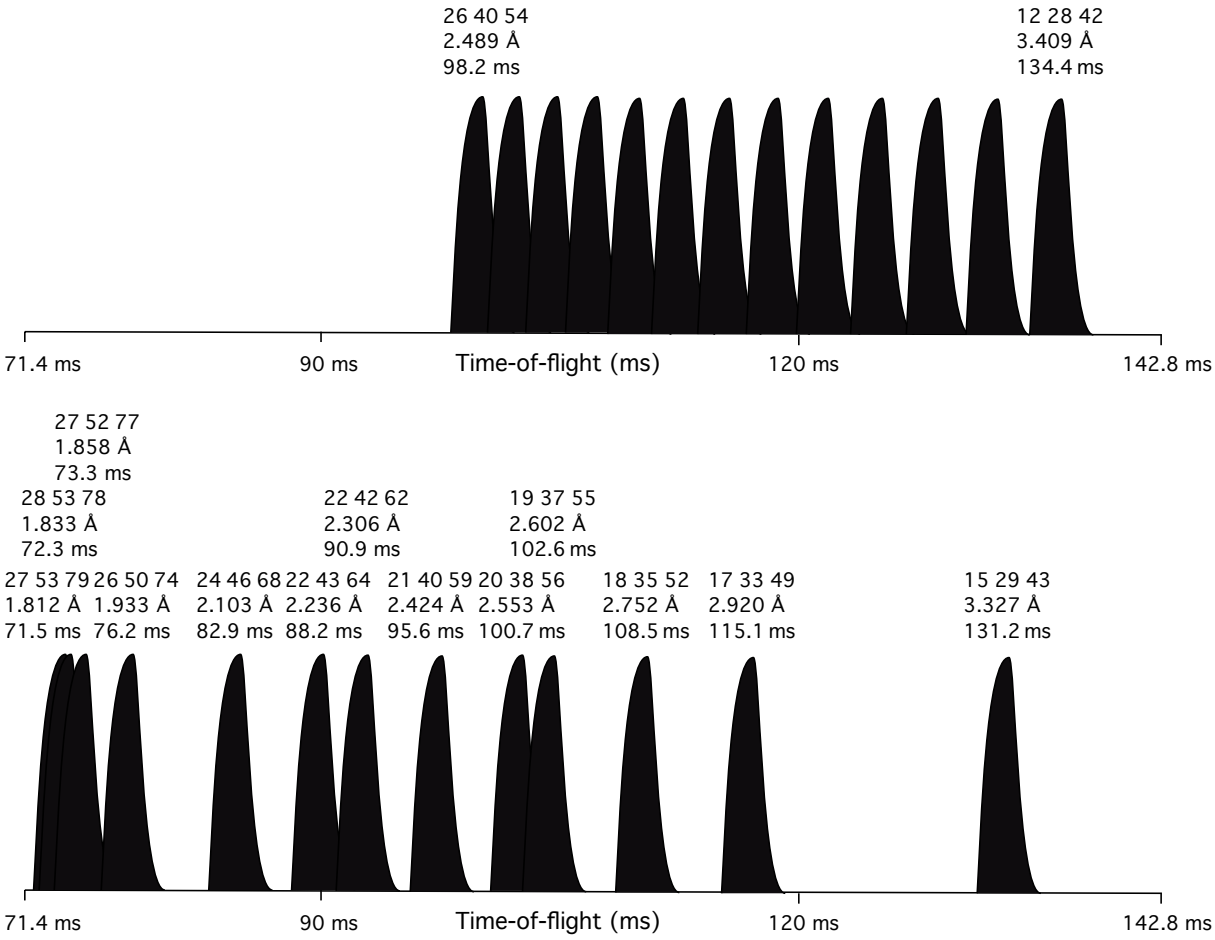

Figure 11 Scale drawing representing the time-of-flight separation of the harmonically (top) and spatially (bottom) overlapped example reflections in bovine heart cytochrome c oxidase.

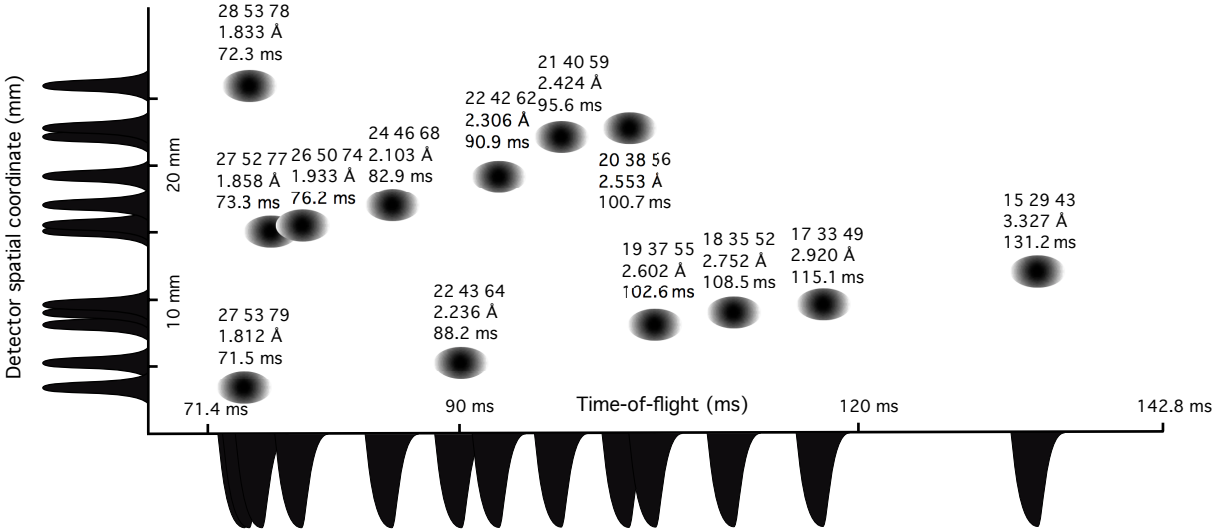

Figure 12 The separation of the spatially overlapped example reflections in Figure 10 in TOF and spatial separation along the approximate zone conic.

The comparative performance of the instrument for materials science applications is naturally best in cases where only relatively small crystals are available. The unit cells of

most inorganic materials are trivial to resolve with this instrument, even when superstructures are present. An example in the ferroelectric LuFe2O4 with a magnetic superstructure that can be described with a unit cell of a=5.94 Å b=10.30 Å c=17.31 Å β=103°, in the space group C2/m. The simulated example magnetic reflections are extremely well resolved both spatially and in TOF (Figure 13). The q-resolution allows possible peak splitting to be observed as well. It is also worth noting that for a given crystal size, the individual reflections from inorganic crystals with moderate unit cells will be much stronger than from a protein crystal. They will also not suffer from the disordered solvent background prominent in macromolecular crystals.

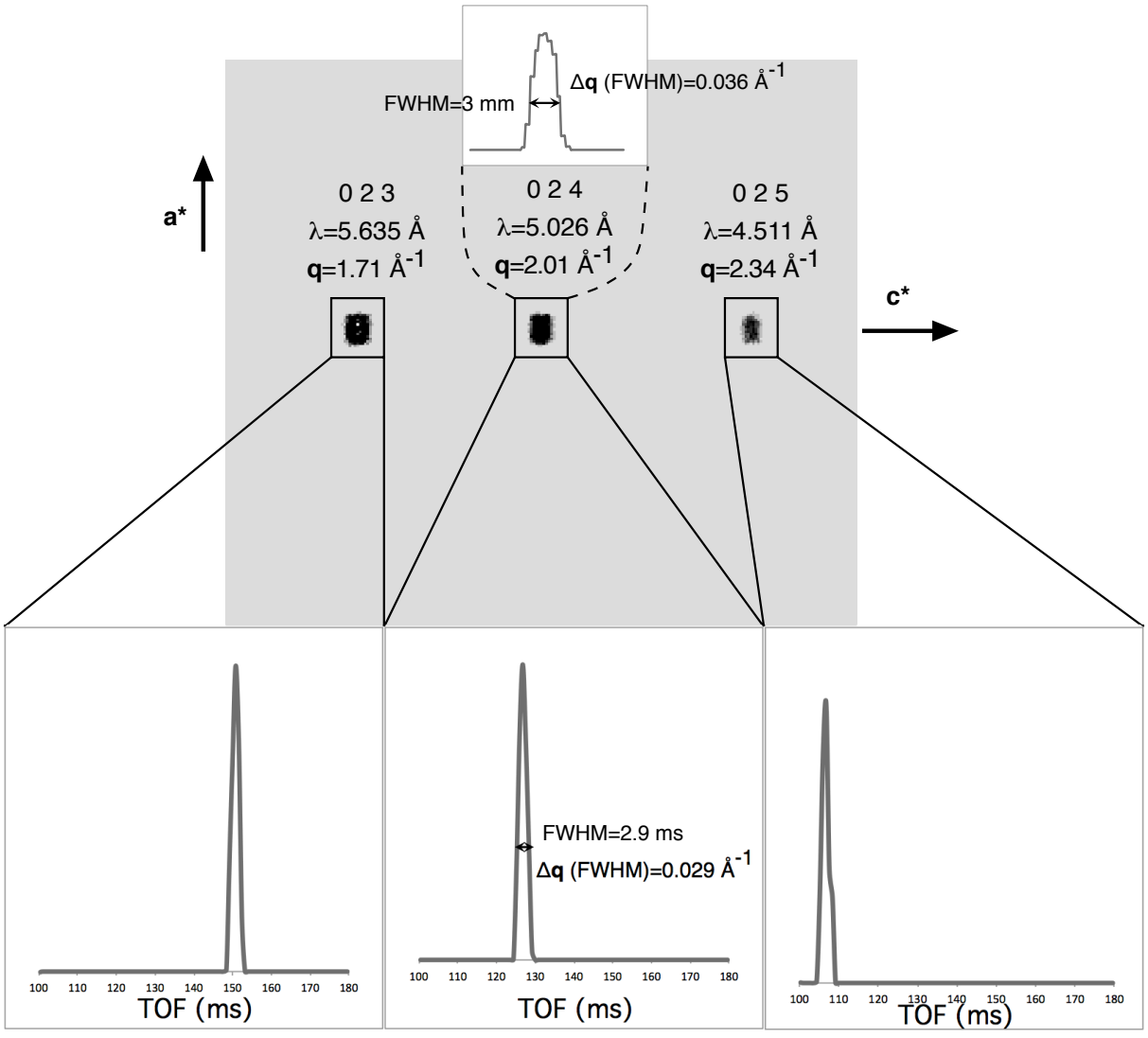

Figure 13 The simulated example magnetic supercell reflections of $LuFe_2O_4$ separated in the spatial (above) and TOF (below) dimensions. The reflections are observed at 2θ =100-114° with a detector distance of 200 mm.

1.4 Strategy and Uniqueness

The macromolecular diffractometer is an instrument dedicated to biological neutron crystallography. The potential user community of protein crystallographers is rather specific to this instrument and has only limited overlap with the rest of the ESS user community. Therefore it is considered as an instrument class of its own. The instrument could also be

used for low-resolution contrast-variation crystallography to study *e.g.* lipid environments of membrane proteins, where the user community overlaps with that of a biological SANS instrument. The materials science community that would use the instrument is likely to also make extensive use of other instruments, such as the Single crystal magnetism diffractometer, General-purpose Polarized SANS, Bispectral Powder diffractometer and various spectrometers.

There are several instruments at other sources dedicated to macromolecular diffraction and some such as D19 at the ILL that are occasionally used for NMX. The current leading instruments are LADI-III at the Institut Laue Langevin (ILL) and the Protein Crystallography Station (PCS) at the Los Alamos Neutron Science Centre (LANSCE). The number of available instruments has increased significantly in recent years with the commissioning of iBIX at the Japan Proton Accelerator Research Centre (J-PARC) and BioDiff at the Forschungsreaktor München II (FRM-II) and the expected commissioning of the Macromolecular Neutron Diffractometer (MaNDi) at the Spallation Neutron Source (SNS) and IMAGINE at the High Flux Isotope Reactor (HFIR) in Oak Ridge will further improve instrument availability. This is a reflection of the growing interest in NMX as more and more scientifically interesting systems can realistically be studied. These instruments all have a fixed detector geometry, posing an inherent limit to the resolvable unit cell edge. The instrument proposed will remove this limitation, provided that the crystal mosaicity is sufficiently low. As the experiments are typically performed at ambient temperature, the inevitable mosaicity increase due to cryo-cooling in X-ray crystallography can be avoided.

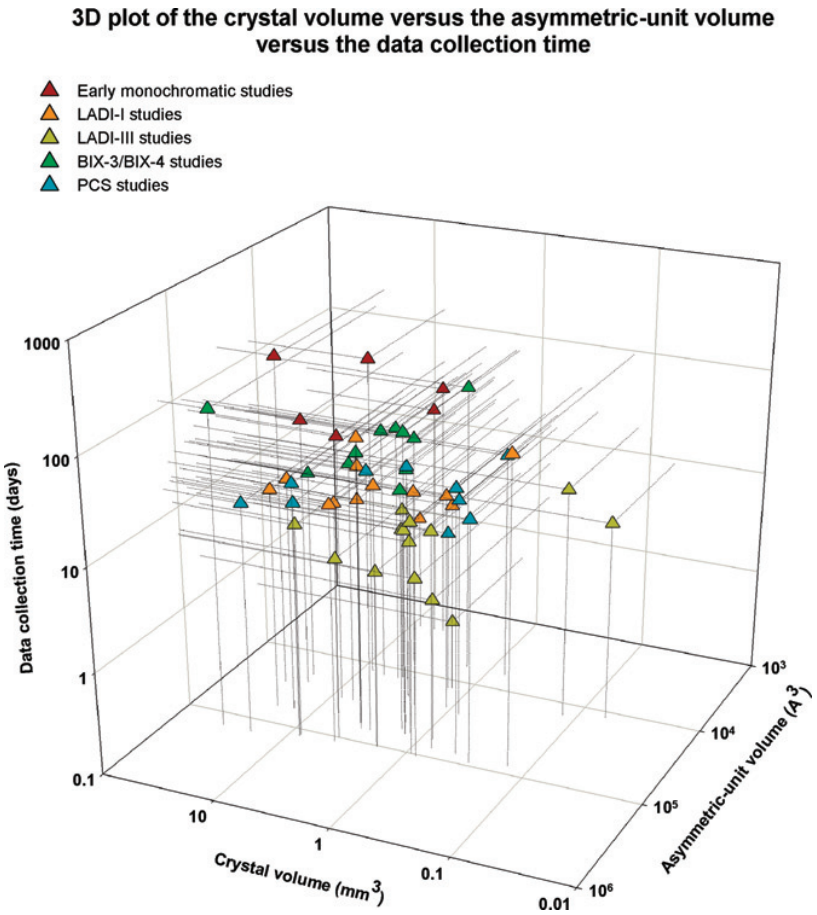

Figure 14 A three-dimensional scatter plot of the asymmetric unit-cell volume versus crystal volume versus data collection time for the various neutron structures solved by 2009 (from Blakeley, M. *Crystallography reviews* 2009 15: 3, 157 — 218*)*.

The limiting factor for NMX and indeed for macromolecular crystallography in general is the size and quality of the crystals that can be obtained and improvements in instrumentation have been pushing that limit towards smaller crystal sizes (Figure 14). In X-ray crystallography the development of microbeams at synchrotron sources has led to a situation where increasing the crystal size beyond ~200 μm offers little advantage. As a consequence, the crystallisation methods are optimised to produce such crystals from a minimal amount of protein material, but not for maximising the diffracting volume, which is required for NMX even with a brilliant source such as the ESS. A state-of-the-art ESS crystallisation facility that develops methods for growing large and well-ordered protein crystals and makes these methods available for the ESS users is therefore an essential factor for the scientific success of a Macromolecular diffractometer. Perdeuteration of the protein material is advantageous for NMX not only for background reduction but also for easier interpretation of the nuclear scattering density maps. It is also important that the ESS support the users in biological deuteration.

In the early years of ESS operations, dedicated instruments will likely not be available for all scientific communities using single crystal diffraction. The proposed instrument could accommodate parts of the science cases of instruments such as SXD at ISIS, TOPAZ at SNS and Cyclops, D19, D10, D9 and D3 at ILL especially when large unit cells and small crystals are involved. Due to the experimental similarities between NMX and magnetic diffraction, the instrument would probably be most useful for magnetic diffraction. Magnetic diffraction users are expected to be an important part of the ESS user community, and this instrument can help engage this community even before a dedicated Single crystal magnetism diffractometer is available.

1.5 Technical Maturity

Feasibility and location

While the proposed instrument concept does not directly resemble any existing instrument, it consists of fairly standard components apart from the detectors. The beam delivery system is relatively simple with a small guide cross-section and low m-value coatings. The technology for achieving sub-millimeter precision for beam and sample positioning is uncommon with neutrons but standard and commercially available for X-ray crystallography. The detector technology is under development by ESS in-kind partners and fallback options are also available.

The instrument would be best placed at southernmost position of the western sector, at the edge of the long instrument hall in the currently proposed layout, allowing space for potential upgrade options.

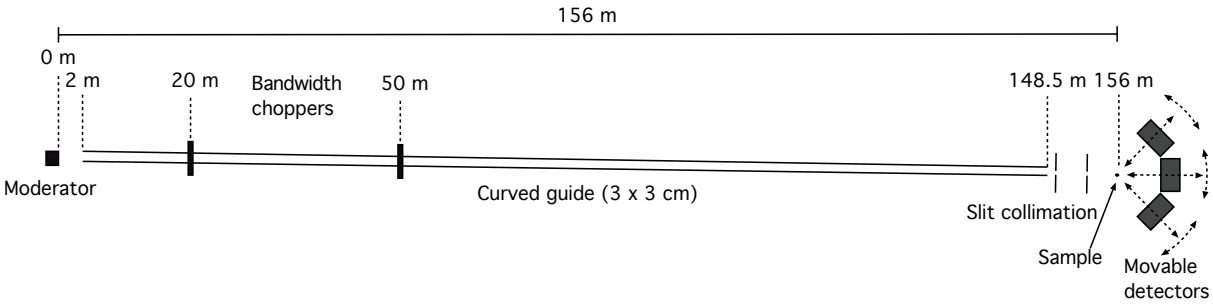

Figure 15 Instrument layout

Detector technology

In terms of technologies to match the required performance, the preferred option is Micro-strip gas chamber (MSGC) detectors coated with gadolinium. They would offer a high position and timing resolution combined with a high detection efficiency in this wavelength range. These are being actively developed for example by Helmholz Zentrum Berlin as part of the ESS in-kind contributions (WU-1.4.2.7.2.2/SD010DE). The present state of the research and development (R+D) is such that the requirements can be matched by this detector technology, however detailed testing of prototypes is needed, in particular relating to operational usage and longevity. The cost and production capacity for such a detector also needs to be evaluated in detail.

Another option is neutron-sensitive semiconductor detectors (as being developed within WU1.4.3.7.2.3/SD053CZ and SD052SE); here various possibilities exist for the readout chip, but the neutron-sensitive semiconductor material needs to be developed further and its performance demonstrated. Here again it is necessary to review the state of advance of the R+D to determine its appropriateness to this instrument.

Lastly, in terms of options for detector technology are the "safe" back-up options. These consist of present-day state-of-the-art options, such as the Anger cameras based upon lithium-glass as the detector medium, such as used by MaNDi at the SNS and wavelength shifting fibre detectors, such as those used by iBIX at JPARC. Even though these back-up options compromise on spatial resolution, they offer safe and low-risk options for detector technology should the R+D for both options above show that they are inappropriate for operational use. As shown above the spatial resolution requirements for the detector depend on the crystal and unit cell size. Therefore a compromise on the spatial resolution would limit the performance with the most challenging cases, but the instrument concept remains valid even using *e.g.* Anger cameras with ~1 mm spatial resolution. All of the technologies discussed above feature a timing resolution that is superior to what is required for this instrument concept.

The detector technologies above are anyway being developed and demonstrated within the ESS design update. The ESS detector group provides resources for these developments. In terms of timeline for review relevant to this instrument proposal, it is proposed as following, to follow all relevant options until they show themselves to be inappropriate. Known events are as follows:

- End-2013: WU-1.4.2.7.2.2/SD010DE (Gd-coated MSGCs) will finish and detailed performance characteristics and estimates of costs and production capacity will be available. This would be a suitable decision point as to whether to continue with development and demonstration of this detector technology.

- End 2014: WU1.4.3.7.2.3/SD053CZ and SD052SE (semiconductors) should have results on feasibility, performance and costs of semiconductor neutron detectors. As such it would be a suitable decision point as to whether to continue with development and demonstration of this detector technology.

The status of developments of all technologies will be reviewed yearly.

Allowing two years for a full and complete demonstration of production modules on instruments and a detailed production plan would allow a final decision on detector technologies before the end of 2016. This rather late decision date ensures that the optimal and most reliable technology is chosen for this instrument. The area of detector coverage is small enough that production should be easily completed within the schedule to be ready for first neutrons in 2019.

Risk management

As discussed above the instrument is largely based on existing technology except for the detectors, so the technological risks are reasonably low. The risks associated with the instrument components and the mitigation of those risk are described below. However, as the estimation of instrument performance and benchmarking is challenging in protein crystallography in general, there is a scientific risk associated with the instrument performance in terms of data collection times and resolvable unit cell edges. This risk will be mitigated by the flexible instrument design that also allows the wavelength band to be shifted towards longer wavelengths if necessary.

There are also generic schedule risks associated with the overall progress of the ESS construction project, but they are not considered here as they do not affect either the scope or budget proposed.

The most significant risks within the beam delivery system are associated with the in-monolith optical components and their lifetime, but since m=1 mirrors are sufficient to transport the necessary brilliance, the eventual replacement of these is not prohibitively costly. The risks associated with optical components are also being considered and mitigated by the ESS neutron optics group. The chopper system for bandwidth selection and frame overlap suppression is established technology and involves low technological risk. The risks associated with choppers are also being considered and mitigated by the ESS chopper group.

There are currently some uncertainties concerning shielding against high-energy neutrons from the target that are being studied by the ESS. At the present planning stage these uncertainties are common to all instruments, but the instrument concept presented here is not particularly sensitive to the potential issues with high-energy background. This is firstly due to the long moderator-to-sample distance and secondly to the fact that the signal to be measured in Bragg peaks is well localised in both scattering angle and time. The background from a ‘prompt pulse’ on the other hand is uniformly distributed in angle. The shielding concepts adopted are not expected to have a major impact on the total shielding cost.

The largest technological risk is associated with the detector technology needed to achieve a spatial resolution of 0.2 mm. Whilst off-the-shelf options do not presently exist, there are various potential technologies under development that could fulfil the specifications. The timeline presently allows sufficient time to be able to fully demonstrate the feasibility and reliability of the technology options; this is in part why it is important that this proposal is in the first round of instrument proposals.

The risk mitigation arising from the strong requirements on specifications for the detector technology is tackled with a two-fold strategy; firstly by check-pointing and reviewing closely and regularly the development and realistic demonstration timeline to be aware of difficulties early; and secondly by ensuring that there are "safe" backup technologies that can still provide adequate performance.

1.6 Costing

The costing presented in Table 1 is indicatively broken down in the four phases of the instrument construction project. The staff effort is estimated in person-months assuming a cost of 10 k€/person-month. The costs are also broken down in the following categories:

Integrated Design: The effort from the Lead Scientist and engineer, as well as other scientists and engineers involved in the overall instrument design

Systems Integration: Systems engineering activities to ensure compatibility between components and compliance with ESS standards.

Detectors and Data Acquisition: Detector systems complete with all electronics. The cost estimates are based on discussions with the ESS Detector group and hardware costs include installation.

Optical Components: The beam delivery system including the guide, the guide housing and alignment system, collimation slits and a focusing nose. The cost estimates are based on a confidential market survey by the ESS Neutron Optics group. The hardware costs include installation.

Choppers: The chopper systems for bandwidth selection and frame overlap suppression. The cost estimates are based on discussions with the ESS Chopper group and hardware costs include installation.

Sample Environment: The goniostat system and humidity control and cryostream systems for sample mounting.

Shielding: The shielding solutions required for radiation protection and background reduction, including shutter systems. The requirements and costing model for the shielding is unclear at the moment, so the current estimate is an engineering estimate from the ESS Neutron Optics group.

Instrument Specific Support Equipment: This includes mechanical components not costed elsewhere.

Instrument Infrastructure: The buildings and facilities not provided as part of the Conventional Facilities budget, such as cabins, mezzanines, raised floor areas etc. As no definite floor plan exists at the moment, the estimate here is based on the costs of the TOPAZ instrument at SNS.

The majority of the costs are incurred in the Procurement and Installation phase, but some of the major procurements could be initiated already in the Final Design phase at the discretion of the Chief Instrument Engineer.

This cost estimate should be regarded as very preliminary and indicative of the relative cost profile between the various components. The uncertainty in the cost estimates can be significantly reduced once a preliminary engineering design is available.

ESS Instrument Proposal

Project Name Macromolecular Diffractometer

Date 16/08/2013

Table 1 Cost estimation

in k€	Phase 1 (Design and Planning)			Phase 2 (Final Design)			Phase 3 (Procurement and Installation)			Phase 4 (Beam Testing and Cold Commissioning)			Total			
	Hard ware	Staff (k€)	Staff (months)	Hard ware	Staff (k€)	Staff (months)	Hard ware	Staff (k€)	Staff (months)	Hard ware	Staff (k€)	Staff (months)	Hard ware	Staff (k€)	Staff (months)	Staff (years)
Integrated Design	0	360	36	0	600	60	0	480	48	0	240	24	0	1680	168	14
Systems Integration	0	0	0	0	30	3	0	120	12	0	60	6	0	210	21	1.75
Detectors and Data Acquisition	0	30	3	0	30	3	5000	60	6	200	120	12	5200	240	24	2
Optical Components	0	30	3	0	30	3	3000	30	3	20	60	6	3020	150	15	1.25
Choppers	0	30	3	0	30	3	700	30	3	20	30	3	720	120	12	1
Sample Environment	0	0	0	0	30	3	500	10	1	20	60	6	520	100	10	0.83
Shielding	0	30	3	0	60	6	3000	60	6	20	60	6	3020	210	21	1.75
Instrument Specific Support Equipment	0	0	0	0	30	3	100	120	12	20	30	3	120	180	18	1.5
Instrument Infrastructure	0	30	3	0	30	3	100	60	6	20	30	3	120	150	15	1.25
Total	0	510	51	0	870	87	12400	970	97	320	690	69	**12720**	**3040**	304	25.3
Grand total (no VAT)	**15760 k€**															
Percentage of			3.2			5.5			84.8			6.4				100

2. LIST OF ABBREVIATIONS

Abbreviation	Explanation of abbreviation
NMX	Neutron macromolecular crystallography
TOF	Time-of-flight
ILL	Institut Laue Langevin, Grenoble, France
PCS	Protein Crystallography Station
LANSCE	Los Alamos Neutron Science Centre
J-PARC	Japan Proton Accelerator Research Centre
FRM-II	Forschungsreaktor München II
SNS	Spallation Neutron Source, Oak Ridge, TN, USA
HFIR	High Flux Isotope Reactor, Oak Ridge, TN, USA
MSGC	Micro-strip gas chamber
R+D	Research and development

PROPOSAL HISTORY

Version	Reason for revision	Date
1.0	New Document	31/10/2012
1.1	STAP and internal review	30/12/2012
1.2	Further comments from the STAP	28/02/2013
1.3	Comments from the SAC	16/08/2013